Design and Analysis of Tracked Robot with Differential Mechanism

Jintao Cui, Ying Wang, Anhong Li, Shuai Shao, Xubing Cai
Department of Information Engineering
Chaoyang Teachers College
Chaoyang, China
jtcui_neu@sina.cn

***Abstract*—A four tracks robot with double rocker arms and differential mechanism is developed. The body of the robot is driven by a single DC motor, and realizes the forward, backward and steering actions by matching with the electromagnetic brakes, and the output power from differential half shafts can be allocated to the double rocker arms, so as to complete the obstacle action. Meanwhile, the obstacle-surmounting performance of step-climbing is analyzed, by establishing the relationship of the inclination angle of the robot, the elevation angle of the swing arm and the height of the step-climbing, the theoretical value of the maximum obstacle height is obtained. And based on the test of the prototype, the measured value of the obstacle height is compared with the theoretical value.**

Keywords—tracked robot; differential mechanism; step-climbing; obstacle-surmounting performance

I. INTRODUCTION

The tracked robot not only has good obstacle surmounting ability and ground adaptability, but suitable for traveling in unstructured terrain, such as natural undulating and rugged terrain, artificial slopes, terraces, ravines and other man-made terrains. Therefore, the mobile robots in the world usually adopts the form of tracked type. As for the research of tracked robot, the United States started earlier, and has developed a series of disaster rescue robots for different purposes. The robotics research center at Carnegie Mellon University developed a detection robot named Groundhog, mainly used for detecting the underground environment and accurately drawing underground stereoscopic maps, the mechanical structure of which adopts four wheel guiding and hydraulic driving, and can realize zero radius turning. Besides, the iRobot company developed a Packbot series of small portable tracked robot, this series of robots adopts the structure of flipper, which can be installed at the front and back ends of the robot according to the requirements of the task, so the robot can overcome obstacles assisted by it, and can be used for battlefield investigation, unknown environment detection and other tasks.

Chinese research for small tracked robot are lagging behind Europe and other developed countries, but in recent years, many universities and research institutes have made many outstanding achievements in scientific research, and continue to narrow the gap with foreign advanced technology. Shenyang Institute of Automation Chinese Academy of Sciences developed a new type of EOD robot, which adopts a wheel, leg and track composite moving mechanism, and the fin-shaped crawlers can rotate around the vehicle body to assist obstacle surmounting, at the same time, the body is equipped with a manipulator, cloud terrace and camera can carry out the operations of grabbing, moving and placing the explosive, which greatly reduces the casualties of the operator in removing the explosive activity. The rescue technology and equipment Research Institute of China University of Mining and Technology successfully developed the first set of mine rescue robot in China in June 2006, named CUMT-I, which adopts four tracks and double rocker arms structure, and can adapt to complex terrain conditions in under-mine, complete underground environmental monitoring, search and rescue tasks.

The tracked robot named TMR-I involved in this paper introduces the differential mechanism into its drive system, that is to say, the robot body is driven by only a DC motor separately. In this way, the number of motors required is reduced, and the robot control system is simplified, so the sensitivity and response speed of the robot are improved. Besides, the mechanism design is simplified, and the weight of the whole machine is reduced, thereby improving the mobility of the robot, and greatly saving the cost.

II. STRUCTURE AND WORKING PRINCIPLE

A. Main Body Structure

The robot mentioned in this paper is shown in figure 1, which maximum shape size is 690×364×151 millimeter, and the total weighs is about 25Kg.

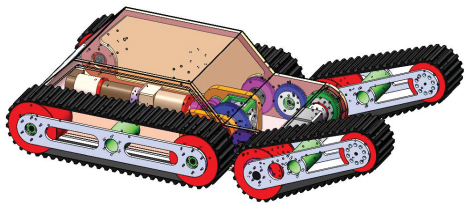

Fig. 1. 3D model of the TMR-I robot

The traction unit of the robot adopts four tracks and double rocker arm structure, by changing the angle of the neutral plane and the horizontal plane of the track, the robot can

The work is supported by the project of national science and technology supporting plan of China (No.2014BAB12B00)

realize the obstacle surmounting, so as to adapt to various unstructured terrain, and the theoretical maximum climbing angle of the robot is 42 degree.

The robot is mainly composed of body 13, differential mechanism 9, main track 17 and rocker arm assembly 18, and the transmission system is shown in figure 2. The main body of the robot is driven by a single DC motor, the model is maxon RE 40, which working voltage is 24V, rated power is 150W, rated output speed is 7850rpm, and the rated output torque is 177mNm. The planetary reducer 10 is capable of reducing speed and generating large torque, thus the output power of the motor may input to the differential mechanism, and finally output by two lines. The first part will input to the driving wheels of the main track assemblies respectively through the left and right shafts of the differential mechanism, so as to drive the main tracks to overcome the ground friction, so that enabling the robot to achieve the forward or backward action. Meanwhile, the second part is output synchronously through the left and right shafts of the differential mechanism, and the driving power is transmitted to the rocker arm drive wheel 3 through the driving gear 7, the intermediate idler 6 and the driven gear 4, and then driving the rocker arm assemblies 18 to operate. Wherein, the intermediate idler wheel 6 is used to ensure that the active tracks 17 and the rocker arms 18 have the same rotation direction. In addition, in order to ensure that the main tracks have the same speed as the rockers, the gears 3, 6 and 7 are designed as spur gears whith same diameter. And the left and right rockers are respectively driven by two stepper motors and relative the body rotates at any angle to realize obstacle surmounting.

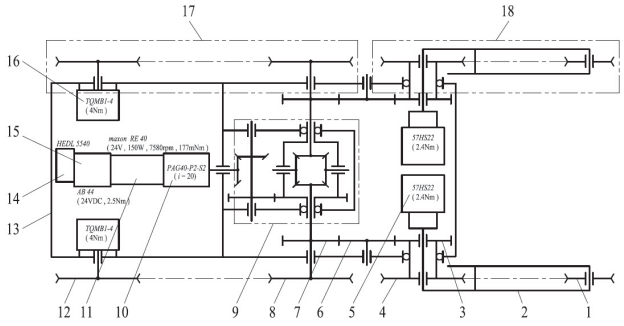

1.driven wheek of the rocker arm ; 2.rocker arm frame ; 3.driven gear ; 4.drive wheel of the rocker arm ; 5.stepper motor ; 6.idle gear ; 7.driving gear ; 8.drive wheel of the main track ; 9.differential mechanism ; 10.planetary reducer ; 11.DC motor ; 12.driven wheel of main track ; 13.frame ; 14.encoder ; 15.main brake ; 16. electromagnetic brake ; 17.main track assembly ; 18.roker arm assembly

Fig. 2. Sketch of the transmission system of TMR-I robot

The forward or backward motion of the robot can be achieved by controlling the forward or reverse rotation of the DC motor. When the robot goes straight, all the brakes are all energized, at this time, the rated speed of the main motor is 7850 rpm, and the total speed reduction ratio of the drive system is 60, so that the speed of the robot is about 2.1kilometer per hour. When the robot turning, take the left turn as an example, the left rear wheel brake of the main track is in a power off state, but the main motor brake and the right rear wheel brake are in the energized state, at this point, the left shaft of the differential is locked, and the power provided by the main motor will all input to the right shaftl, so as to drive the robot to realize the left turn, and the the rotating center is the contact point of the left rear wheel and the ground. In summary, the disadvantage of this design is that the robot needs to overcome the larger ground resistance, and then put forward higher requirements for the working ability of the main motor.

B. Differential mechanism

The main drive system of TMR-I tracked robot adopts the ordinary bevel gear differential, and the working principle is shown in figure 3, obviously, the power of the DC motor through the planetary gear reducer, bevel gears 1, 2 and spur gear 3, 4 driving the differential shell H to rotate, and then through the planetary gear 5, 7 and drive gear 6, 8 and finally output through the left and right semi driving shafts.

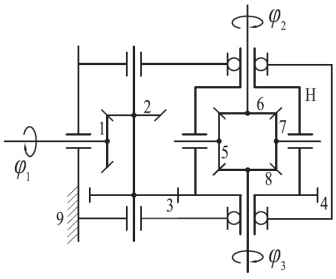

Fig. 3. Working principle of bevel gear differential mechanism

When the robot keeps moving in a straight line, both sides of the track wheel are subjected to the same surface resistance, and react on the two meshing point of the planetary gear through the semi shafts and the gears. At this point, the planetary gears correspond to an equal armed lever, and the planetary gear does not rotate but rotates along with the differential shell and there are no rotational speed difference between the planetary gear shaft and the two shafts, that is $n_1=n_2=n_0$, $n_1+n_2=2n_0$. At the same time, the torque of the main DC motor M_0 is passed to the differential shell, and then be divided into left and right drive shafts, that is $M_1=M_2=M_0/2$.

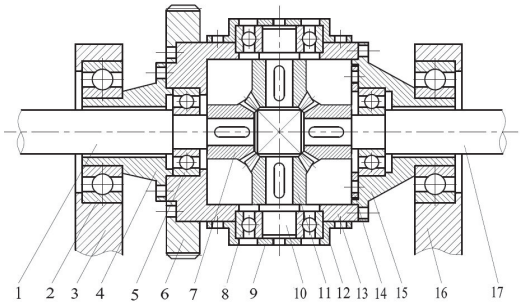

1. left drive shaft ; 2, 5, 8. bearing ; 3, 16.body ; 4. left supporting shaft ; 6. driven gear ; 7, 11. bevel gear ; 9.platen ; 10. planetary shaft ; 12.bearing seat ; 13. differential carrier ; 14. bearing plate ; 15. right supporting shaft ; 17. right drive shaft

Fig. 4. Structure of bevel gear differential mechanism

When the robot turns to the left, the left main track wheel has a higher ground resistance than the right wheel. The two resistances, by driving the drive axle and the half shaft gear,

react to the meshing point of the planetary gear, so that the planetary gear rotates clockwise in addition to the revolution of the differential case, and the rotation speed is n_4. At this time, the gear speed of the left half shaft gear decreases, while the speed of the right one increases, and the increase of the rotational speed of the right half gear is equal to Δn, which is equal to the reduction of the left one, that is, $n_1=n_0-\Delta n$, $n_2=n_0+\Delta n$, there is still exist the relation of $n_1+n_2=2n_0$. Due to the revolution of the planetary gear, it is affected by the friction torque M_T, so that the gear torque of the left half shaft increases, and the torque of the right one decreases, that is, $M_1=(M_0-M_T)/2$, $M_2=(M_0+M_T)/2$. Because the actual M_T is too small to be ignored, there is $M_1=M_2=M_0/2$.

III. Centroid Distribution Analysis

Set up the coordinate system xO_1y which takes the axis of the driven wheel of the main track as the coordinate origin. As shown in Figure 5, define the center distance O_1O_2 of the two pulleys of the main track as l_0, the quality of the body is m1, and the center of mass coordinates $G_1(l_1, h)$. The quality of the rocker unit is m_2, the centroid coordinates G_2, located above the center line of rocker O_3O_4, and the center distance of the main driving wheel is l_2, the angle between the center line O_3O_4 and line O_1O_3 is θ, and $\theta \in (0, 2\pi)$. Besides, the center distance between the main drive wheel and the rocker arm drive wheel is defined as d, and the radius of the main track drive wheel is R, the radius of the rocker arm drive wheel is r (both of which include the track thickness), and the structural parameters of the robot are shown in Table I.

TABLE I. Structural Parameters of the Robot

Structural parameter	value	Structural parameter	value
l_0/mm	300	r/mm	71.500
l_1/mm	195.250	d/mm	120
h_1/mm	41.083	m_1/Kg	10.354
l_2/mm	75.500	m_2/Kg	2.153
R/mm	91.500	/	/

According to the motion theory on center of mass [10]

$$\vec{r}_c = \Sigma m_i \vec{r}_i \Big/ \Sigma m_i \tag{1}$$

Then the centroid coordinates of the robot $G(x_G, y_G)$ are

$$\begin{cases} x_G = \dfrac{m_1 l_1 + m_2 (l_0 + d)}{m_1 + m_2} + \dfrac{m_2 l_2}{m_1 + m_2} \cos\theta \\ y_G = \dfrac{m_1 h_1}{m_1 + m_2} + \dfrac{m_2 l_2}{m_1 + m_2} \sin\theta \end{cases} \tag{2}$$

Obviously, the robot centroid coordinates satisfy the following relations

$$[x_G - \frac{m_1 l_1 + m_2 (l_0 + d)}{m_1 + m_2}]^2 + [y_G - \frac{m_1 h_1}{m_1 + m_2}]^2 = (\frac{m_2 l_2}{m_1 + m_2})^2 \tag{3}$$

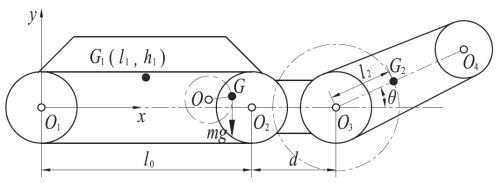

Fig. 5. The centroid trajectory of the TMR-I robot

IV. Obstacle Surmounting Performance Analysis

The process of the robot climbs the steps is shown in figure 6, by controlling the phase angle of the stepping motor of the rocker arms, which initial elevation angle can be set, in order to make contact with the outside line level of the step. When the main tracks drive the robot forward, by controlling the step motor to change the elevation angle of the rocker arms, the inclination angle of the main body of the robot can be changed, then makes the front end of the main tracks lean on the outside line level of the step. With the increasing of α, the gravity center of the main body moves forward continuously, and when it crosses the vertical face of the step, the robot will take the outside line level of the step as its pivot and make a flat turn along it, and then realize climbing over.

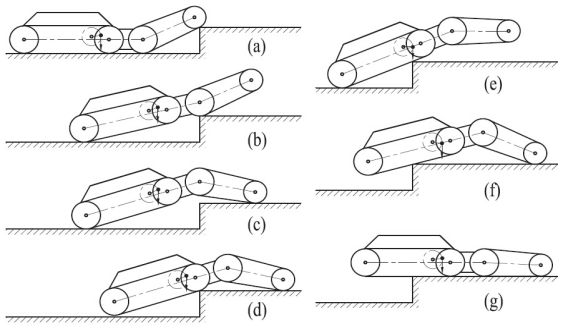

Fig.6. Step-climbing process of the TMR-I robot

As shown in Figure 7, The gravity center of the robot coincides with the vertical face of the step, and when the center line of the rocker arm is kept horizontal, it is the critical state for the robot to cross a step. At this point, The climbing capacity of a robot exists maximum value. Obviously, the dip angle of the body and rocker elevation have the following relationship.

$$\alpha + \theta = 2\pi \tag{4}$$

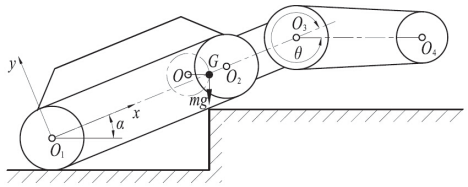

Fig.7. Critical state of the step-climbing process

Then the step height that the robot can climb is

$$H(\theta,\ \alpha)=R+x_{\mathrm{G}}\sin\alpha+y_{\mathrm{G}}\cos\alpha-(y_{\mathrm{G}}+R)\sec\alpha \qquad (5)$$

In order to determine the monotonicity of the step height function H(θ, α) and whether there is an extremum, the first and second rank partial derivatives of the dip angle α are solved respectively.

$$\frac{\partial H}{\partial\alpha}=x_{\mathrm{G}}\cos\alpha-y_{\mathrm{G}}\sin\alpha-\frac{(y_{\mathrm{G}}+R)\sin\alpha}{\cos^{2}\alpha} \qquad (6)$$

$$\frac{\partial^{2}H}{\partial\alpha^{2}}=-x_{\mathrm{G}}\sin\alpha-y_{\mathrm{G}}\cos\alpha-(y_{\mathrm{G}}+R)\frac{\sin^{2}\alpha+\cos\alpha}{\cos^{3}\alpha} \qquad (7)$$

Because $\alpha\in(0,\ \pi/2)$, so $\partial^2H/\partial\alpha^2<0$. At this point there is a maximum value of $H(\theta,\ \alpha)$, and when $\partial^2H/\partial\alpha^2=0$, $H(\theta,\ \alpha)$ has a maximum value of $H_{\max}$.

The structural parameters of the robot in Table 1 are brought into formula (2) and (5), so that the climbing height equation of the robot can be obtained.

$$\begin{aligned}H(\theta,\ \alpha)=&0.0915+(0.234+0.013\cos\theta)\sin\alpha+(0.034\\&+0.013\sin\theta)\cos\alpha-(0.126+0.013\sin\theta)\sec\alpha\end{aligned} \qquad (8)$$

In the above formula $\alpha\in(0,\ \pi/2)$ and $\theta\in(0,\ 2\pi)$, using the MATLAB software to fit formula (8), the relationship of the climbing step height $H(\theta,\ \alpha)$, the elevation angle of the rocker arms θ, and the dip angle of the main body α can be obtained, which is shown in Figure 8. The calculation results show that when α=42°, θ=318°, $H_{\max}(\theta,\ \alpha)$= 214.3mm. That is, the maximum step height of the robot can climb is 214.3mm, and there is $\alpha+\theta$=360°, Obviously, this is consistent with the analytical result of formula (4).

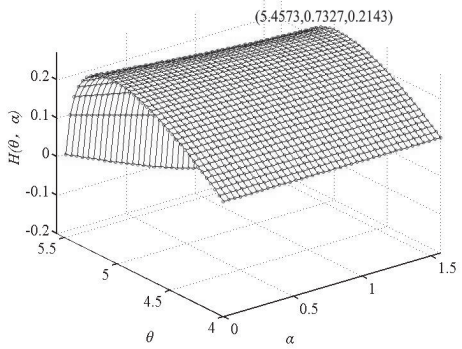

Fig.8. The relationship of the inclination angle of the robot, the elevation angle of the swing arm and the height of the step-climbing

In addition, in order to test the obstacle performance of TMR-I robot, a field test on the prototype was implmented, as shown in Figure 9, the measured height that the robot can climb is 220mm, which verifies the correctness of the theoretical analysis.

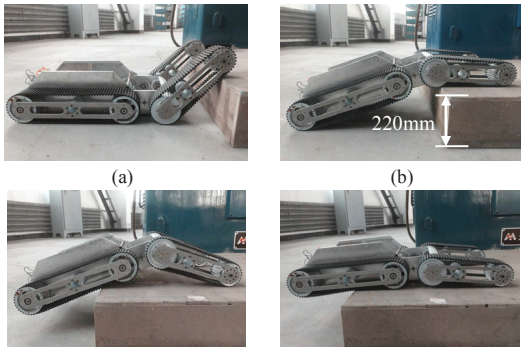

Fig.9. The obstacle-surmounting ability tests of the TMR-I robot prototype

V. CONCLUSION

The differential mechanism is introduced to the design of the transmission mechanism of the robot, that is, the robot body is driven by a single DC motor, which simplifies the control system, enhances mobility and reduces weight and costs. At the same time, the obstacle surmounting performance is analyzed according to the center of mass motion, thus the maximum theoretical height of obstacle crossing is obtained. Finally, the field test of the prototype is carried out, which proved that the measured obstacle crossing height is consistent with the theoretical value.

REFERENCES

[1] H.R. Choi, S.M. Ryew, "Robotic system with active steering capability for internal inspection of urban gas pipelines", Mechatronics, Vol.16 , pp. 713-736, 2002.

[2] B.S. Choi, S.M. Song, "Fully automated obstacle-crossing gaits for walking machines", IEEE Transactions on Systems, Man and Cybernetics, Vol.18, pp. 952-964, 1998.

[3] J.G. Liu, Y.S. Wang, S.G. Ma, "Analysis of stairs-climbing ability for a tracked reconfigurable modular robot", IEEE International Workshop on Safety, Security and Rescue Robotics,Piscataway, NJ, USA, IEEE, pp. 36-41, 2005.

[4] S.G. Roh, H.R. Choi, "Differential-drive in-pipe robot formoving inside urban gas pipeline", IEEE Transactions on Robotics, Vol. 21, pp.1-17, 2005.

[5] S.H. Qian, S.R. Ge, Y.S. Wang, "Research status of the disaster rescue robot and its applications to the mine rescue", Robot, Vol.28, pp.350-354, 2006.

[6] L. Huang, T.H. Lee, "Position force control o f unce rtain constrained flexible joint robots", Mechatronics, Vol.16, pp. 111-120, 2006.

[7] D. Sun, "Position synchronization of multiple motion axes with adaptive coupling control", Automatica, Vol.39, pp. 997-1005, 2003.

[8] J.G. Xin, X.F. Li, Z. Wang, "Performance analysis of track-leg mobile robot in unstructured environment", Robot, Vol.22, pp. 35-39, 2004.

[9] D.S. Chen, Y. Hang, T.M. Wang, "Obstacle climbing analysis and simulation of wheel-legged robot", Journal of Beijing Univer sityof Ae ronautics and Astronautics , Vol.35, pp.371-375, 2009.

[10] D.P. Miller, L. Tan, S. Swindell, "Simplified navigation and traverse planning for a long-range planetaryrove",IEEEInternational Conference on Robotics and Automation. Piscataway, NJ, USA: IEEE, pp.2436-2441, 2003.